Noninvasive Monitoring of Gene Transfer Using a Reporter Receptor Imaged with a High-Affinity Peptide Radiolabeled with ^{99m}Tc or ^{188}Re

Kurt R. Zinn, Donald J. Buchsbaum, Tandra R. Chaudhuri, James M. Mountz, William E. Grizzle, and Buck E. Rogers

Departments of Radiology, Radiation Oncology, and Pathology, University of Alabama at Birmingham, Birmingham, Alabama

Gene therapy protocols require better modalities to monitor the location and level of transferred gene expression. One potential in vivo mechanism to assess gene expression would be to image the binding of a radiolabeled peptide to a reporter receptor that is expressed in targeted tissues. This concept was tested in a tumor model using a replication-incompetent adenoviral vector encoding the human type 2 somatostatin receptor (Ad5-CMVhSSTr2). Expression of the hSSTr2 reporter was imaged using a radiolabeled, somatostatin-avid peptide (P829). **Methods:** Bilateral subcutaneous A427 tumor xenografts were established on the flanks of athymic nude mice. These human-origin, non–small cell lung tumors are normally negative for hSSTr2 expression. One tumor was injected directly with Ad5-CMVhSSTr2, whereas the second tumor was injected directly with a control Ad5 vector. The mice were injected intravenously 48 h later with P829 peptide that was radiolabeled to high specific activity with ^{99m}Tc (half-life, 6 h) or ^{188}Re (half-life, 17 h). Tumors were frozen and evaluated for somatostatin receptor expression using fluorescein-labeled somatostatin. **Results:** The accumulation of radiolabeled P829 in hSSTr2-expressing tumors was easily visualized by γ camera imaging 3 h after injection. Imaging region of interest analyses and biodistribution studies confirmed a 5- to 10-fold greater accumulation of both radiolabeled P829 peptides in the Ad5-CMVhSSTr2-injected tumors versus control tumors injected with control Ad5 vectors. Ad5-CMVhSSTr2-injected tumors accumulated 2.5–3.8 percentage injected dose per gram 3 h after injection. Only Ad5-CMVhSSTr2-injected tumors expressed somatostatin receptors, as determined by immunohistochemistry. **Conclusion:** These studies show the feasibility of imaging a ^{99m}Tc-labeled peptide's binding to a reporter receptor after in vivo gene transfer to tumor cells. The ^{188}Re-labeled peptide worked equally well for this imaging approach and offers the additional advantage of energetic β decay with potential therapeutic efficacy. ^{99m}Tc and ^{188}Re are generator produced, an advantage for widespread availability and low cost, and both radioisotopes can be imaged with existing, high-resolution modalities. There is great potential for using ^{99m}Tc-labeled peptides for imaging gene transfer with the hSSTr2 reporter receptor, especially when the reporter correlates with the expression of therapeutic genes that can be included simultaneously in the gene therapy vector.

Received May 7, 1999; revision accepted Sep. 14, 1999.

For correspondence or reprints contact: Kurt R. Zinn, DVM, PhD, University of Alabama at Birmingham, Dept. of Radiology, Division of Nuclear Medicine, BDB 11, 1530 3rd Ave. S., Birmingham, AL 35294-0012.

Key Words: imaging; gene transfer; somatostatin receptor; peptide; ^{99m}Tc; ^{188}Re

J Nucl Med 2000; 41:887–895

The development of noninvasive and sensitive techniques to image gene expression will positively impact the future of gene therapy aimed at treating human diseases (*1–4*). Reporters based on enzymatic systems (luciferase or β-galactosidase), fluorescent markers (green fluorescent protein or derivatives), or detection of protein products using immunohistochemistry are excellent indicators of the expression of transferred genes in vitro. Certain light-based reporters are capable of measuring gene transfer noninvasively in the retina (*5*) or in rodent disease models (*6,7*). Fluorescent probes that are activated by a transferred gene product, though not yet described, are a logical extension of the approach used by Weissleder et al. (*8*). However, these light-based reporter systems are limited in their capability for widespread evaluation of gene transfer to entire organ systems or targeted disease in humans (e.g., cancer). Light-based reporter systems for in vivo imaging are surface techniques.

Most reports of noninvasive, in vivo imaging of gene transfer are based on a common mechanism: the accumulation of an intravenously injected, radiolabeled compound at the location of gene transfer and expression. An image representing the distribution of the radiolabeled compound is reconstructed, after externally detecting the γ rays using γ camera, SPECT, or PET imaging techniques. The first successful demonstration of in vivo imaging of gene transfer in an animal tumor model followed transfer of the herpes simplex virus 1 thymidine kinase gene (HSTK) (*9–11*). HSTK phosphorylates ganciclovir (a nontoxic prodrug) into a toxic, trapped metabolite capable of killing the tumor cell. By injecting a radiolabeled derivative of the prodrug (5-[^{131}I]-2′-deoxy-2′-fluoro-β-D-arabinofuranosyl-5-iodouracil [FIAU]), HSTK-expressing tumor cells were detected by measuring the local accumulation of radioactivity by γ camera and SPECT imaging. This same approach for imaging gene transfer was extended to PET using specific ^{18}F-labeled prodrug derivatives (*12–16*). A substrate specific

for mammalian thymidine kinase 1, 3′-deoxy-3′-[^{18}F]fluorothymidine, was also applied for imaging cell proliferation with PET (*17*). Cell proliferation can also be imaged by PET using 5-[^{124}I]iodo-2′-deoxyuridine (*18*).

An alternate approach to the enzymatic-based reporter system uses a reporter receptor, the in vivo expression of which can be imaged by specific binding of its radiolabeled ligand, agonist, or antagonist. One example of this approach used a transplantable tumor stably expressing the type 2 dopamine receptor (D_2R). After implantation in nude mice, the D_2R-positive tumors were imaged with an ^{18}F-labeled dopamine receptor antagonist, 3-(2′-[^{18}F]fluoroethyl)spiperone (FESP) (*16,19,20*). An additional report, though more indirect, involved in vitro studies by Weissleder et al. (*21*), in which the binding of ^{111}In to melanin was detected by imaging the cell culture dishes after transfer of the tyrosinase gene. None of these reports involved in vivo administration of vectors used in gene therapy.

This study investigated the feasibility of using the human type 2 somatostatin receptor (hSSTr2) as a reporter receptor for imaging gene transfer. An adenoviral vector encoding the hSSTr2 gene under control of the cytomegalovirus (CMV) promoter (Ad5-CMVhSSTr2) was constructed to test this concept. A427 cells (human non–small cell lung, hSSTr2 negative) were infected with the Ad5-CMVhSSTr2, either in vitro for binding assays or after implantation and tumor growth in athymic nude mice. In this study, expression of the transferred hSSTr2 gene was imaged noninvasively with a γ camera using a ^{99m}Tc- and a ^{188}Re-labeled somatostatin analog (P829; Diatide, Inc., Londonderry, NH), which is a synthetic peptide with high affinity for hSSTr2 (*22,23*). Imaging data correlated with biodistribution data and indicated a high sensitivity for imaging gene transfer by this approach.

^{99m}Tc-labeled P829 has a proven efficacy for detection of somatostatin-positive tumors in animal models (*22,23*) and somatostatin-positive lung and breast tumors in humans (*24,25*). The U.S. Food and Drug Administration approved the drug in August 1999. The usefulness of ^{99m}Tc-labeled P829 to image expression of the hSSTr2 reporter gene can now be tested in human gene therapy trials. The advantages of ^{99m}Tc relative to other radioisotopes that might be applied to this approach include high specific activity, short half-life (6 h), low dose associated with the mode of decay (no β emission), constant availability from generators, low cost, abundant low-energy γ-ray emission (140 keV, 90%), and widespread availability of γ cameras required for imaging with this radioisotope. ^{188}Re, which has radiolabeling chemistry similar to that of ^{99m}Tc, also is obtained from a generator at high specific activity. It has a half-life of 17 h and can be imaged with its 15% abundant 155-keV γ-ray emission. Because ^{188}Re decays by β emission (maximum binding capacity [B_{max}] = 2.1 MeV), it is capable of delivering a radiotherapy dose to somatostatin-receptor positive tumors.

MATERIALS AND METHODS

Cell Lines and Adenovirus

The A427 (non–small cell lung cancer) and NCI-H69 (small cell lung cancer) cells, as well as the 293 human transformed primary embryonal kidney cells, were obtained from the American Type Culture Collection (Rockville, MD). Cells were grown in Eagle's minimum essential medium containing nonessential amino acids and 1 mmol/L sodium pyruvate supplemented with 10% fetal bovine serum. The cells were cultured at 37°C in a humidified atmosphere with 5% CO_2 until ready for use. The replication-incompetent adenoviral vector encoding hSSTr2 complementary DNA under the control of the CMV promoter element (Ad5-CMVhSSTr2) was produced and purified as described (*26*). The recombinant adenovirus was plaque purified, validated by the polymerase chain reaction, and titered within 293 cells using plaque assay techniques for direct determination of viral plaque-forming units (pfu). The replication-incompetent adenoviral vector encoding *Escherichia coli* β-galactosidase under control of the CMV promoter element (Ad5-CMVLacZ) was obtained from De-chu Tang (University of Alabama at Birmingham, Birmingham, AL). The replication-incompetent adenoviral vector encoding thyrotropin-releasing hormone receptor under control of the CMV promoter element (Ad5-CMVTRHR) was obtained from Erik Falck-Pedersen (*27*).

Radiolabeling

Chemicals were from Fisher (Pittsburgh, PA) unless otherwise noted. P829 kits containing 50 μg peptide, 0.1 mg disodium ethylenediaminetetraacetic acid dihydrate (EDTA), 5 mg sodium glucoheptonate dihydrate, and 50 μg $SnCl_2$ dihydrate were provided by Diatide. The P829 kit was injected with 1 mL saline containing 92 or 185 MBq $^{99m}TcO_4^-$ (Central Pharmacy, Birmingham, AL) and boiled for 10 min. The same protocol was followed for radiolabeling with $^{188}ReO_4^-$ (92 MBq added), except an additional 1.0 mg $SnCl_2$ was added and boiling time was 15 min. The final solution was filtered through a 0.2-μm filter into a vial containing gentisic acid (1 mg) as an antioxidant. ^{188}Re was obtained by elution of a ^{188}W/^{188}Re generator obtained from Oak Ridge National Laboratory (Oak Ridge, TN) (*28,29*). The radiolabeled P829 peptides were subjected to high-performance liquid chromatography (HPLC) and instant thin-layer chromatography (ITLC) analyses. The ITLC silica gel strips (Gelman Sciences, Inc., Ann Arbor, MI) were spotted with the radiolabeled P829 peptide at 1 end and eluted with either saturated saline, methyl ethyl ketone, or a 50:50 mixture of methanol and ammonium acetate (1 mol/L) as the mobile phase. The strips were imaged with a γ camera after elution. P829-bound ^{99m}Tc and ^{188}Re did not migrate with either saturated saline or methyl ethyl ketone. The radiolabeled P829 migrated only with the mixture of methanol and ammonium acetate. For HPLC analyses, the radiolabeled P829 peptides were injected on a Zorbax C_{18} column (Mac-Mod Analytical, Chadds Ford, PA) equilibrated with 0.1% trifluoroacetic acid. A gradient of 20%–27% acetonitrile (0.1% trifluoroacetic acid) over 30 min resulted in elution of the radiolabeled P829 at 19 min with radiometric detection.

Scatchard Analysis

Binding characteristics of ^{99m}Tc-P829 and ^{188}Re-P829 were studied by Scatchard analysis using A427 membrane preparations from uninfected cells and cells infected with Ad5-CMVhSSTr2 at 10 pfu/cell. A427 cells at ~80% confluency were infected with

Ad5-CMVhSSTr2 at 10 pfu/cell in Optimem (Gibco-BRL, Grand Island, NY) and incubated for 2 h at 37°C in 5% CO_2. The cells were supplemented with complete media, incubated an additional 48 h at 37°C, and harvested to make cell membranes as described (*26*). The membranes (10–30 μg) were diluted in buffer (10 mmol/L N-[2-hydroxyethyl]piperazine-N'-[2-ethanesulfonic acid], 5 mmol/L $MgCl_2$, 1 mmol/L EDTA, 0.1% bovine serum albumin [BSA], 10 μg/mL leupeptin, 10 μg/mL pepstatin, 0.5 μg/mL aprotinin, and 200 μg/mL bacitracin, pH 7.4), and 100 μL were added to each well of a Multiscreen Durapore filtration plate (type FB, 1.0-μm borosilicate glass fiber over 1.2-μm Durapore membrane; Millipore, Bedford, MA) and filtered. Various concentrations of ^{99m}Tc-P829 or ^{188}Re-P829 were added, with or without a 1000-fold molar excess of unlabeled P829 as a blocking agent, to the membranes such that the final concentrations of the radiolabeled peptides ranged from 0.1 to 15 nmol/L. The samples were incubated at room temperature (RT) for 60 min, washed twice with ice-cold buffer, and allowed to dry; the individual wells were punched out and counted in a γ counter. The data were analyzed using the National Institutes of Health (NIH) Ligand program (*30*).

Internalization Assay

A427 cells at ~80% confluency were infected with Ad5-CMVhSSTr2 at 10 pfu/cell 48 h before addition of ^{99m}Tc-P829 or ^{188}Re-P829 at a final concentration of ~0.8 nmol/L. Uninfected A427 cells were used as negative controls, and a 1000-fold molar excess of unlabeled P829 was used to determine specific binding and internalization. At 1 or 4 h after addition of ^{99m}Tc-P829 or ^{188}Re-P829, the medium was aspirated, the cells were washed with Hanks' balanced salt solution (HBSS) containing 20 mmol/L sodium acetate (pH 4.0) to remove surface-bound radioactivity and were harvested to determine the amount of internalized radioactivity. Data are presented as the specific amount of radioactivity surface bound or internalized as a percentage of the total radioactivity added.

A similar, independent assay was conducted by adding 5 nmol/L fluorescein-labeled somatostatin (Fluo-somatostatin; New England Nuclear, Boston, MA) to uninfected A427 cells or A427 cells infected with Ad5-CMVhSSTr2 at 100 pfu/cell with incubation at 37°C. Two hours after addition of Fluo-somatostatin, the cells were trypsinized and resuspended in HBSS (containing 0.1% NaN_3 and 1% BSA). Viable cells (10,000/sample) were analyzed by fluorescence-activated cell sorting using a FACS Scan (Becton Dickinson, Mountain View, CA).

Animal Tumor Model

Animal protocols were reviewed and approved by the Institutional Animal Care and Use Committee of the University of Alabama. Female athymic nude mice (~20 g) were obtained from the National Cancer Institute Frederick Research Laboratory (Frederick, MD) and inoculated with 2×10^6 A427 cells (1:1 mixture with Matrigel) subcutaneously on each rear flank. Fourteen days later, 1 tumor (~0.2 g) was injected directly with Ad5-CMVhSSTr2, whereas the other tumor was injected directly with a control adenovirus, either Ad5-CMVLacZ or Ad5-CMVTRHR. The amount of Ad5 vector injected directly into the tumors was 10^9 or 10^{10} pfu for mice injected intravenously 48 h later with ^{99m}Tc-P829 and 10^9 pfu for mice injected intravenously 48 h later with ^{188}Re-P829. ^{99m}Tc-P829-injected groups (5.5-MBq dose) contained 3 mice per group, the ^{99m}Tc-P829-injected group (9-MBq dose) contained 4 mice, and ^{188}Re-P829-injected groups consisted of 6 mice. Additional mice (n = 10) were also implanted with NCI-H69 cells (human small cell lung cancer), a tumor line that was known to be positive for hSSTr2. These mice were not injected with adenoviral vectors.

Biodistribution Studies

Two days after the Ad5 injections, the mice were injected with ^{99m}Tc-P829 or ^{188}Re-P829. There were 2 different doses of ^{99m}Tc-P829, either 5.5 MBq (0.15 μg) or 9 MBq (0.5 μg); only 1 dose of ^{188}Re-P829 was administered (9 MBq, 0.6 μg). Intravenous injections into the tail vein were accomplished under halothane anesthesia. Syringes were counted before and after injection using an Atomlab 100-dose calibrator (Biodex Medical Systems, Shirley, NY) to determine the exact dose. When the animals were killed, the tissues were collected, weighed, and counted in a Minaxi Auto-Gamma 5000 series γ counter (Packard Instrument Co., Downers Grove, IL). After the tissues were removed, the remaining carcass was subdivided into vials for counting. Statistical comparisons used ANOVA protocols in the Statistical Analysis System (SAS, release 6.11; SAS Institute Inc., Cary, NC).

Imaging and Region of Interest Analyses

The mice were imaged with an Anger 420/550 mobile radioisotope γ camera (Technicare, Solon, OH) equipped with a pinhole collimator. Intrinsic resolution of the detector was 3.3 mm. Mice were imaged initially and 3 h after injection using planar imaging techniques. During imaging, the mice were maintained with halothane anesthesia and positioned in ventral recumbency with the legs extended from the body. For single-image sessions at least 50,000 total counts per image were collected. Image acquisition time ranged from 3 to 10 min, with the longer time required for imaging ^{188}Re-P829. The tumor weight for all animals averaged 0.19 ± 0.02 g at the time of imaging.

Images were processed on a Pegasys computer processing system (ADAC Laboratories, Milpitas, CA) or with a modified version of NIH Image (NucMed_Image; Mark D. Wittry, St. Louis University) using standard region of interest (ROI) analyses. ROIs included tumor, kidney, and whole animal. A background region was drawn outside the animal image to correct the whole-mouse, kidney, and tumor ROIs. Total counts and pixels were recorded for all regions. The average counts per pixel for the background region were multiplied by the pixels in the whole-animal and tumor ROIs; that number was then subtracted from the counts in each respective region to yield the actual count values for the whole animal and tumor. The fraction of activity in the tumor region was calculated as the ratio between the background-corrected counts in the tumor region divided by the initial (immediately after intravenous injection) background-corrected counts in the whole animal.

Immunohistochemistry

A separate group of mice (n = 4) bearing 14-d A427 tumor xenografts was injected (intratumor, 10^9 pfu) with either Ad5-CMVhSSTr2 or Ad5-CMVTRHR. After 2 d the mice were killed. Both tumors were cut into pieces and frozen in TissueTek OCT (Miles, Inc., Elkhart, IN). Six-micron frozen sections were cut, mounted on Plus slides, and stored at −20°C for up to 3 d. The slides were incubated at RT in HBSS containing 0.001% phenol, 0.1% glucose, 1% BSA, and 40 mg/L bacitracin for 30 min. Fluo-somatostatin was diluted with the above-modified HBSS to 30 μmol/L immediately before use. The HBSS was drained from the slides, and the somatostatin peptide was added to the tissue sections for 2 h at RT in humidity chambers. Aqueous 3% H_2O_2 was added for 5 min to quench endogenous peroxidase. After rinsing

with HBSS, 3% goat serum in PBE buffer (1 g bovine serum albumin, 0.0292 g EDTA, 0.00975 g NaN_3, added to 100 mL PBS; pH adjusted to 7.6) was applied for 20 min at RT as a nonspecific block (*31*). The goat serum was drained and replaced by 10 or 20 μg/mL antifluorescein (rabbit polyclonal, antifluorescein biotin conjugate [Molecular Probes, Inc., Eugene, OR]) in PBE buffer, and the frozen sections were incubated for 1 h at RT. The slides were rinsed 3 times (2 min each) with tris buffer and fixed for 1 h with neutral buffered formalin. The biotinylated antibody was localized with Ultra Streptavidin Peroxidase (Signet Laboratories, Dedham, MA) for 20 min. The chromogen used was 3,3′-diaminobenzidine (BioGenex, San Ramon, CA). The tissues were counterstained with hematoxylin for 1 min, washed with running tap water for 4 min, and dehydrated with graded alcohols (70%–95%), absolute ethanol, and xylenes (3 times) for 5 min each and mounted with Permount (Fisher).

RESULTS

Radiolabeling of P829 and In Vitro Analyses

The P829 peptide was radiolabeled with ^{99m}Tc and ^{188}Re at high specific activity (18–36 MBq/μg protein) and the radiochemical purity of each was >95% by ITLC and HPLC analyses. The equilibrium dissociation constant (K_d) determined from the Scatchard analyses for ^{99m}Tc-P829 (n = 3) binding to cell membranes from A427 cells infected with Ad5-CMVhSSTr2 was 7 ± 1 nmol/L, whereas the K_d for ^{188}Re-P829 (n = 2) was 6.0 ± 2 nmol/L (Fig. 1). The B_{max} values determined with ^{99m}Tc-P829 and ^{188}Re-P829 were similar (129 and 122 fmol/μg protein, respectively). Because of the lack of hSSTr2 on uninfected A427 cells, the K_d and B_{max} values could not be determined.

For the internalization assay, the amount of surface-bound ^{99m}Tc-P829 was similar 1 or 4 h (3.3% and 3.1%, respectively) after addition of the radiolabeled peptide to A427 cells infected with Ad5-CMVhSSTr2 48 h previously (Fig. 2). This compared with 4.0% and 2.5% of ^{188}Re-P829 being surface bound at 1 and 4 h, respectively. The internalization of ^{99m}Tc-P829 and ^{188}Re-P829 into A427 cells infected 48 h earlier was similar at 1 and 4 h after addition of the radiolabeled peptides. ^{99m}Tc-P829 had 1.7% and 9.2% internalized at 1 and 4 h, respectively, compared with 1.2% and 9.9% for ^{188}Re-P829. Uninfected A427 cells had <0.4% of the radioactivity bound or internalized at 1 or 4 h for either radiolabeled peptide (data not shown). By flow cytometry analyses, uninfected A427 cells incubated with Fluo-somatostatin had a mean fluorescence intensity of 3.0. This value was substantially lower than that of cells infected with Ad5-CMVhSSTr2 at 100 pfu/cell, which had a mean fluorescence intensity of 27.7.

Imaging and Biodistribution of ^{99m}Tc-P829

The γ camera imaging position and location of the subcutaneous tumors are shown in Figure 3A. Representative images are presented for ^{99m}Tc-P829 (5.5 MBq, 0.15 μg) at 3 min after intravenous injection (Fig. 3B) and at 3 h (Fig. 3C) in 3 mice bearing A427 tumors that were injected directly 48 h earlier with either Ad5-CMVhSSTr2 or Ad5-CMVLacZ. The tumors injected with the Ad5-CMVhSSTr2 showed accumulation of ^{99m}Tc-P829 and were visible on the images. The Ad5-CMVLacZ-injected tumors did not show accumulation of the tracer. The images show the blood clearance of the peptide with high uptake in the kidneys. The uptake of ^{99m}Tc-P829 was measured by ROI analyses; data are summarized in Figure 3D. For both adenovirus doses there was approximately a 5- to 10-fold higher accumulation of the radiotracer in Ad5-CMVhSSTr2-injected tumors compared with that in Ad5-CMVLacZ-injected tumors. By ROI analyses, the percentage injected dose (%ID) per tumor ROI in the Ad5-CMVhSSTr2-injected group (10^9 pfu) was 0.9 ± 0.1 %ID in contrast to the Ad5-CMVLacZ-injected group (10^9 pfu) at 0.22 ± 0.06 %ID. Tumors injected with the higher viral titer of Ad5-CMVhSSTr2 (10^{10} pfu) showed statistically significant ($P < 0.05$) higher uptake of ^{99m}Tc-P829 in the tumor ROI (1.5 ± 0.2 %ID/tumor-ROI) compared with the lower Ad5-CMVhSSTr2 dose.

In an additional experiment, mice (n = 4) were injected with a 3-fold higher mass of ^{99m}Tc-P829 (9 MBq, 0.5 μg).

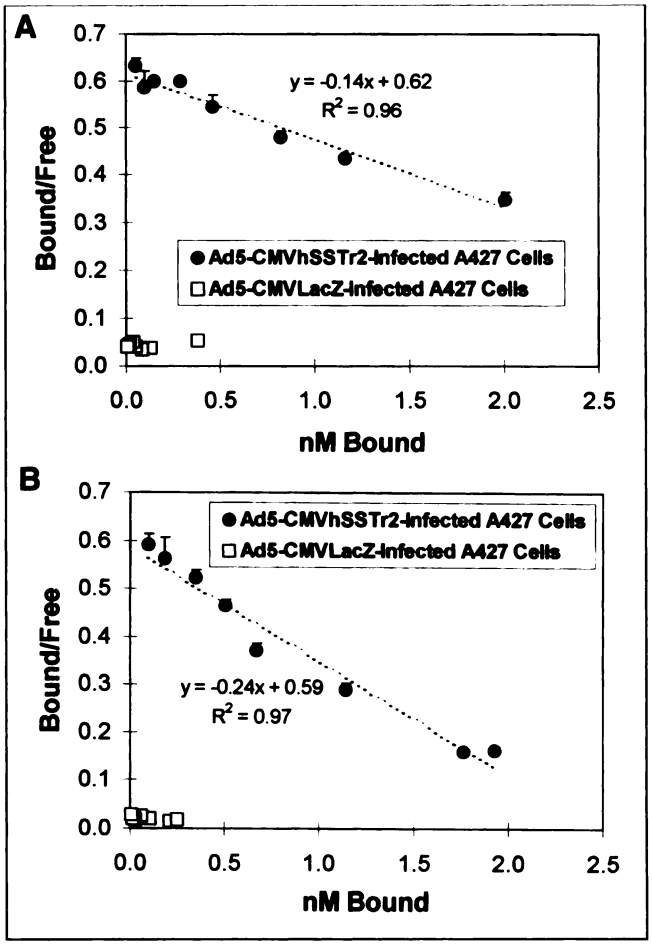

FIGURE 1. Scatchard analyses. Representative plots of ^{99m}Tc-P829 (A) and ^{188}Re-P829 (B) binding to A427 cells (membrane preparations) that were infected with Ad5-CMVhSSTr2 or Ad5-CMVLacZ. Specific high-affinity binding was shown only for Ad5-CMVhSSTr2-infected cells. K_d values for ^{99m}Tc-P829 and ^{188}Re-P829 averaged 7 and 6 nmol/L, respectively.

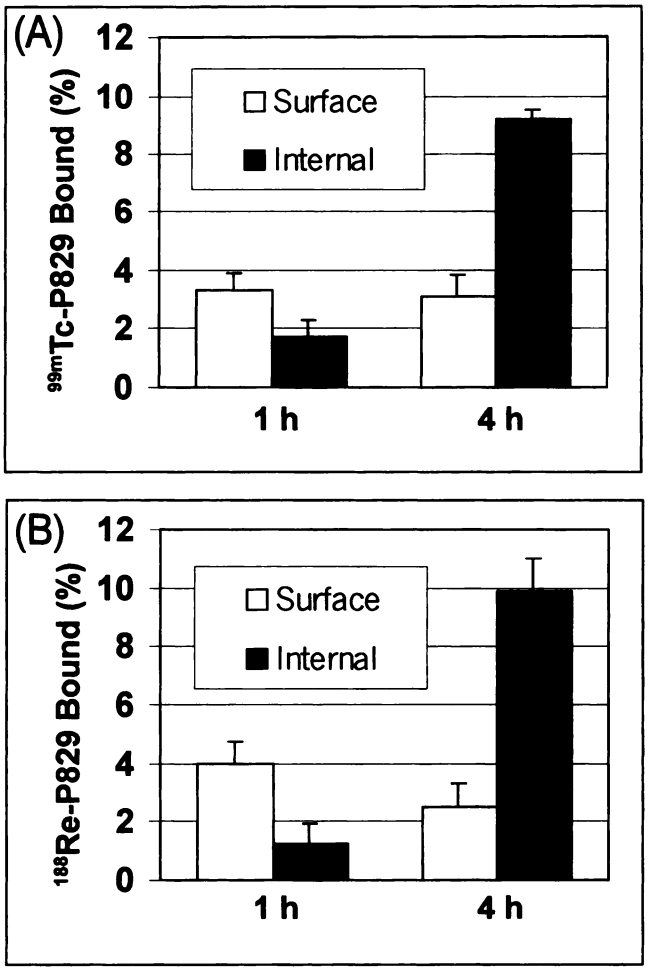

FIGURE 2. Internalization assays. Data shown are means ± SEM for ^{99m}Tc-P829 (A) and ^{188}Re-P829 (B) using A427 cells that were infected with Ad5-CMVhSSTr2. Statistically significant internalization was shown at 4 h for both radiolabeled peptides.

This experiment compared Ad5-CMVhSSTr2-injected tumors with Ad5-CMVTRHR-injected control tumors at 48 h after direct injection of 10^9 pfu. ROI analyses of the 3-h images showed a ^{99m}Tc-P829 accumulation that was identical with that found for the lower ^{99m}Tc-P829 dose (0.15 μg). Tumor uptakes averaged 0.9 ± 0.1 %ID/tumor-ROI in Ad5-CMVhSSTr2-injected tumors and 0.1 ± 0.02 %ID/tumor-ROI in the control, Ad5-CMVTRHR-injected tumors.

The mice were killed and organs were collected for individual analyses after the 3-h imaging session. Results of these analyses are presented in Figure 4. Uptakes of ^{99m}Tc-P829 in tumor (%ID/g) are presented in Figure 4A for mice injected 48 h earlier with the adenoviral vectors. There was excellent agreement between the increased uptake of ^{99m}Tc-P829 in the Ad5-CMVhSSTr2-injected tumors by direct measurement (Fig. 4A) and imaging ROI analyses (Fig. 3D). For mice injected with ^{99m}Tc-P829 at 48 h after Ad5 doses, the uptake in Ad5-CMVhSSTr2-injected tumors ranged from 2.5 to 3.8 %ID/g. The uptake in Ad5-CMVLacZ-injected tumors in the same mice was approximately 10-fold less, at 0.4 ± 0.1 %ID/g. Uptake results from mice bearing another xenograft, human lung tumor (NCI-H69, naturally hSSTr positive), are included in Figures 4A for comparison. This comparison shows that Ad5-mediated transfer of hSSTr2 to A427 tumors (normally hSSTr2 negative) resulted in hSSTr2 levels that were higher than the hSSTr levels normally found on NCI-H69 tumor cells because the tumor uptake of ^{99m}Tc-P829 (0.6 ± 0.1 %ID/g, n = 10) was significantly lower ($P < 0.05$). Although not included with the data presented in Figure 4, the higher dose of ^{99m}Tc-P829 (0.5 μg) resulted in similar tumor uptake. Ad5-CMVhSSTr2-injected tumors accumulated 3.1 ± 1 %ID/g, whereas the control Ad5-CMVTRHR-injected tumors averaged 0.5 ± 0.04 %ID/g.

Figure 4B presents the uptake of ^{99m}Tc-P829 in normal tissues in the mice. The kidney, which showed the highest accumulation, is not included on the graph. Kidney binding was dose dependent, averaging 165 ± 10 %ID/g for the lower dose of ^{99m}Tc-P829 (0.15 μg) and increasing to 210 ± 10 %ID/g for the higher dose ^{99m}Tc-P829 (0.5 μg). The uptake in kidney, as determined by ROI analyses, was in complete agreement with the uptake determined by remov-

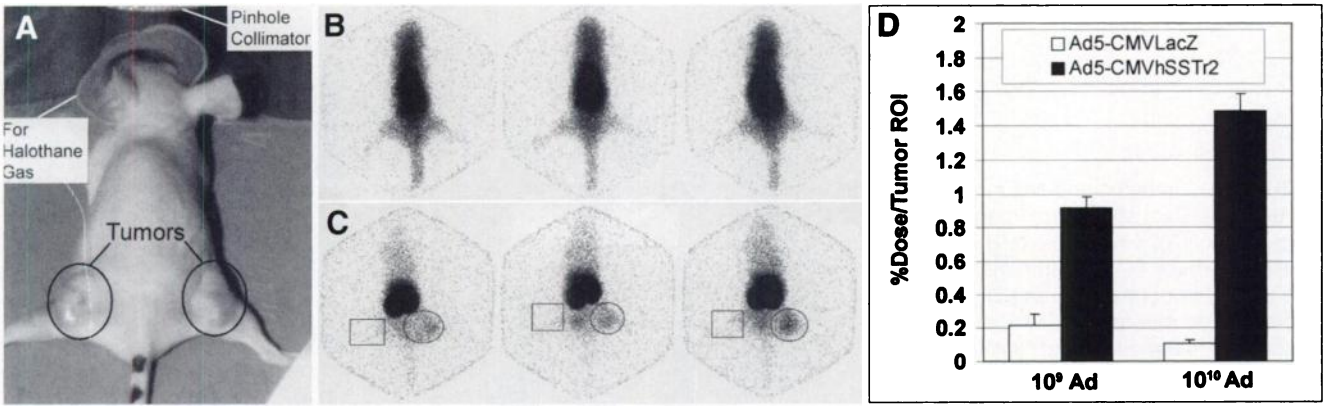

FIGURE 3. γ camera imaging of mice injected with ^{99m}Tc-P829. Imaging position is shown in (A), with 3 representative images of mice at 3 min (B) and 3 h (C) after intravenous injection. Circles in (C) indicate location of human A427 tumors injected 48 h earlier with Ad5-CMVhSSTr2, and squares indicate human A427 tumors injected 48 h earlier with Ad5-CMVLacZ. (D) Results of ROI analyses. Ad = adenovirus.

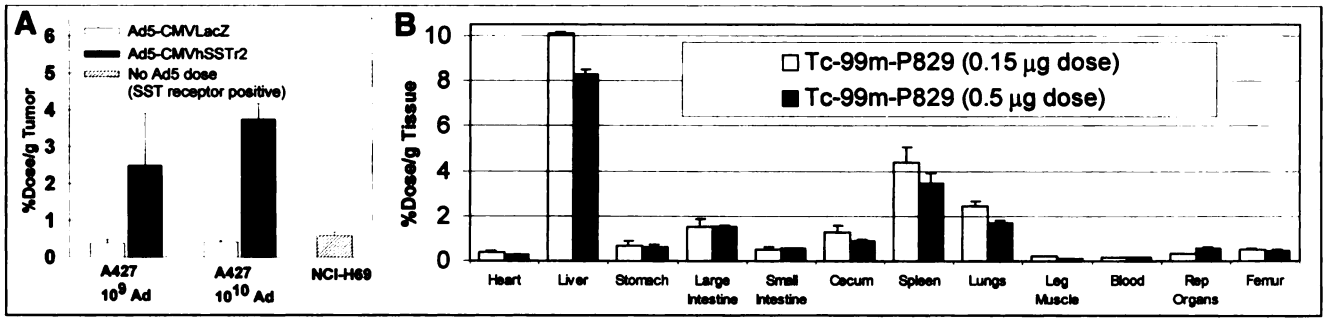

FIGURE 4. Uptake of ^{99m}Tc-P829 by γ counter analyses. Data shown are means ± SEM at 3 h after intravenous injection in tumors (A) and normal tissues (B). NCI-H69 (hSSTr2-positive tumor) is included for comparison. Each mouse had 2 tumors that were injected directly with either Ad5-CMVhSSTr2 or Ad5-CMVLacZ (1×10^9 pfu/tumor). ^{99m}Tc-P829 was injected 48 h after Ad5 vector injections.

ing and counting the organ in a γ counter. The tissues with significant uptake (highest to lowest) were kidney, liver, spleen, and lungs. The latter 3 tissues showed lower uptake of ^{99m}Tc-P829 with the higher dose. All other tissues had relatively low uptake of ^{99m}Tc-P829.

Imaging and Biodistribution of ^{188}Re-P829

Images are presented in Figure 5 for ^{188}Re-P829 after intravenous dosing (9 MBq, 0.6 μg) in mice bearing A427 tumors that were injected directly 48 h earlier with either Ad5-CMVhSSTr2 or Ad5-CMVLacZ. Similar to the ^{99m}Tc-labeled peptide, the ^{188}Re-labeled P829 showed high uptake in the kidneys at 3 h. Tumors injected with Ad5-CMVhSSTr2 showed accumulation of ^{188}Re-P829 and were visible on the images. Ad5-CMVLacZ-injected tumors did not show accumulation of the ^{188}Re-P829.

Figure 5B presents the results (n = 6 mice) of ROI analyses from imaging as well as γ counter analyses after removing the tumors when the animals were killed. The uptake of ^{188}Re-P829 in Ad5-CMVhSSSTr2-injected tumors averaged 1.6 ± 0.1 %ID/tumor-ROI or 2.9 ± 0.8 %ID/g (γ counter). In contrast, the uptake in control, Ad5-CMVTRHR-injected tumors was 0.4 ± 0.0 5 %ID/tumor-ROI or 0.3 ± 0.05 %ID/g (γ counter). These results are similar to those presented for ^{99m}Tc-P829. The uptakes of ^{188}Re-P829 in

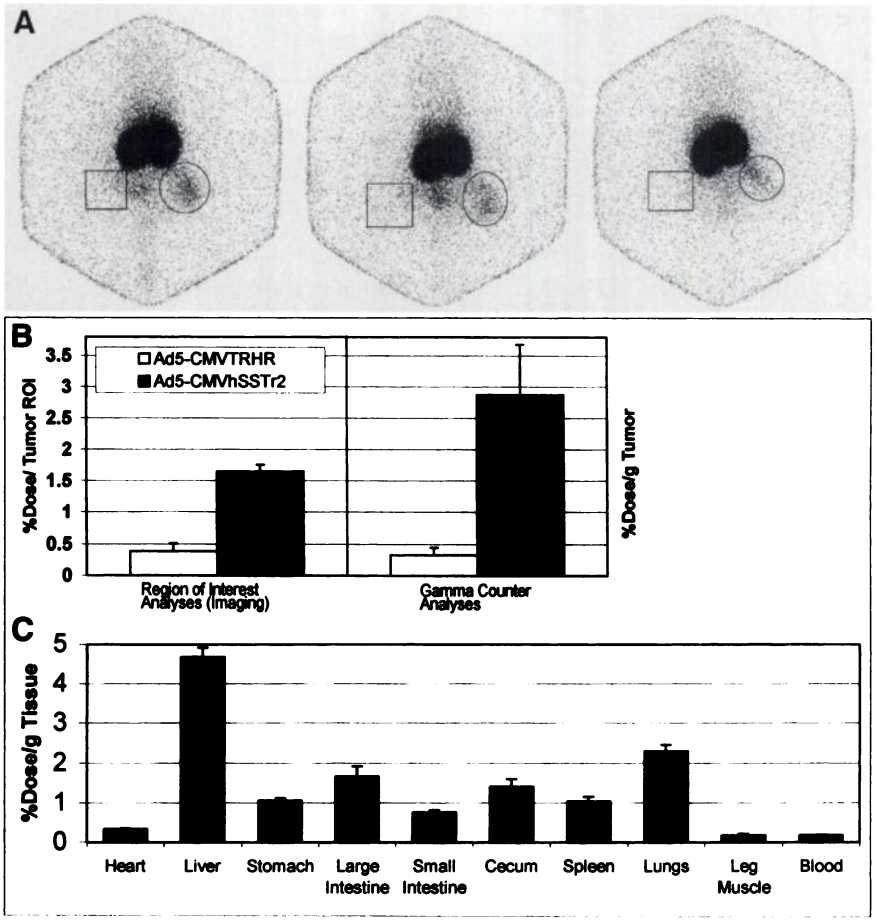

FIGURE 5. Imaging and tissue uptake of ^{188}Re-P829. Data shown are images at 3 h after dosing (A), tumor uptake determined by ROI analyses or γ counter analyses (B), and uptake in normal tissues (C). Data are expressed as means ± SEM. Circles in (A) indicate location of human A427 tumors injected 48 h earlier with Ad5-CMVhSSTr2, and squares indicate human A427 tumors injected 48 h earlier with Ad5-CMVTRHR. ^{188}Re-P829 was injected intravenously 48 h after Ad5 vector injections, and mice were imaged and killed at 3 h.

other tissues are presented in Figure 5C. These data show that ^{188}Re-P829 had lower accumulation in liver, spleen, and lungs compared with ^{99m}Tc-P829 (Fig. 4C). The kidneys, which are not included in Figure 4C, showed accumulation of 187 ± 10 %ID/g, which was similar to the results obtained with ^{99m}Tc-P829.

Immunohistochemistry

After imaging, the tumors were removed and analyzed by immunohistochemistry. Ad5-CMVTRHR-injected tumors showed minimal background staining, primarily in scattered macrophages. Ad5-CMVhSSTr2-injected tumors showed cells expressing somatostatin receptors in 3 of the 4 tumors that were examined. Of interest, the negative tumors had low uptake of the radiolabeled peptide (data not shown). The location of the positive areas appeared to be along the Ad5 needle tract and at the termination of the probable injection site. In addition, areas of necrosis were noted frequently at the terminations of the probable injection tracts for the Ad5-CMVhSSTr2-injected tumors. Figure 6A shows cells expressing somatostatin receptor along an apparent injection tract. Figure 6B shows no staining in a similarly stained frozen section from the matching control tumor from the same mouse.

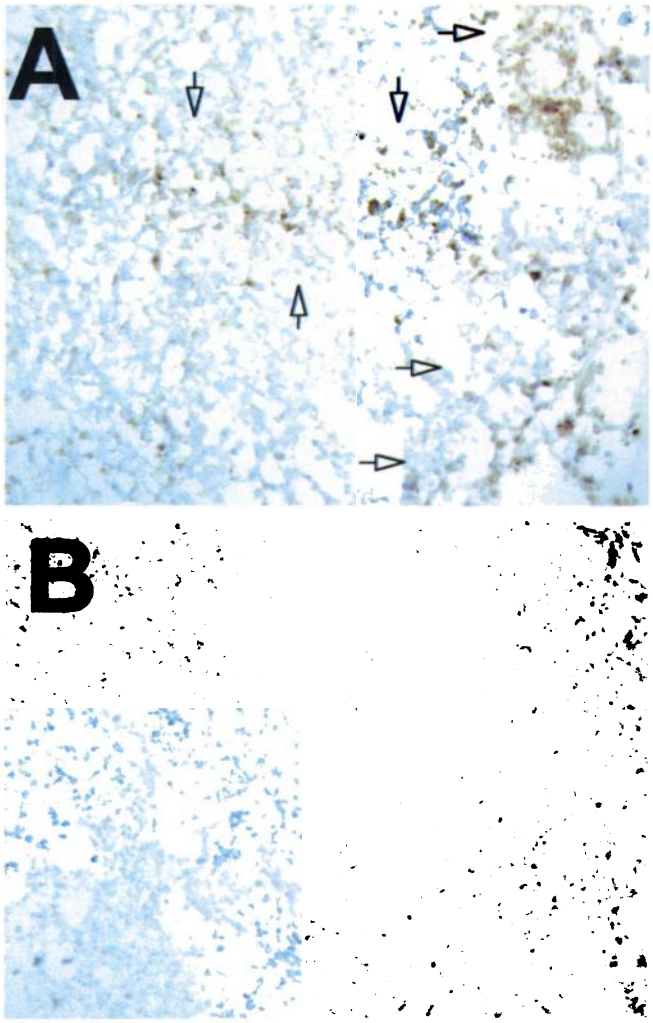

FIGURE 6. Immunohistochemistry of adenovirus-injected tumor xenografts. Stained frozen sections (×200) are from Ad5-CMVhSSTr2-injected tumor, which shows cells expressing somatostatin receptors along apparent injection tract (A, arrows) (necrosis is at apparent end of tract, upper and lower arrows) and Ad5-CMVTRHR-injected tumor from same mouse as in (A) showing only scattered macrophage staining (B).

DISCUSSION

These studies have shown that P829 peptide was efficiently labeled with both ^{99m}Tc and ^{188}Re in a manner that retained specific, high-affinity binding to the type 2 somatostatin receptor. Internalization assays showed a disappearance of bound peptide (^{99m}Tc or ^{188}Re labeled) from the surface of Ad5-CMVhSSTr2-infected cells, with increasing intracellular accumulation over time. Specific internalization of fluorescein-labeled somatostatin was also shown by flow cytometry. The accumulation of P829 in the tumor cells over time may be an important aspect of high sensitivity for imaging (^{99m}Tc-P829) and delivery of a therapeutic dose (^{188}Re-P829).

The expression of hSSTr2 resulting from Ad5-mediated transfer to A427 tumors (by direct injection) was imaged after injection of either ^{99m}Tc- or ^{188}Re-P829 peptides. This capability provided a noninvasive assessment of the level and extent of gene transfer and was confirmed by immunohistochemistry. One index of the sensitivity of the technique is the tumor uptake (%ID/g), which reached 3.8 and 2.9 %ID/g for ^{99m}Tc-P829 and ^{188}Re-P829, respectively. This uptake was higher than that found for a naturally hSSTr2-positive xenograft tumor, which showed levels of 0.6 ± 0.1 %ID/g. The uptake of radiolabeled P829 in tumors (%ID/g) was also greater than that reported for the accumulation ^{131}I-FIAU in subcutaneous tumors injected with HSTK-expressing cells (*10*). The reported values in the studies by Tjuvajev et al. (*10*) were typically in the range of 0.2–1 %ID/g, with the highest value at 1.3 %ID/g. Further studies with subcutaneous tumors injected with HSTK-expressing cells by Tjuvajev et al. (*11*), using ^{124}I-FIAU, showed tumor accumulations of 0.1–0.2 %ID/g at 50 h, 10-fold higher than that of negative tumors. The ^{124}I-FIAU allowed PET imaging at high resolution and showed heterogeneous expression of the HSTK in the tumor. PET imaging (using ^{18}F-FESP) was also used to repeatedly image tumors expressing a stable D_2R transgene (*20*). These studies (*11,20*) suggest that future clinical trials will benefit from a high-resolution technique for imaging gene transfer. A combination of SPECT with the hSSTr2 reporter, ^{99m}Tc-P829 system described here would provide an alternative, high-resolution and high-sensitivity approach.

The uptake of ^{99m}Tc-P829 in the Ad5-CMVhSSTr2-injected tumors was used to estimate the number of hSSTr2 receptors produced per Ad5-infected cell. For the purpose of these calculations, it was assumed ^{99m}Tc-P829 and unlabeled P829 had similar binding affinity for the hSSTr2 receptor. On the basis of this assumption, a tumor uptake of 1% of the

^{99m}Tc-P829 (total dose = 0.5 μg), as determined from imaging ROI analyses, would equal 10^{12} total P829 molecules. From cell culture studies it was determined that 40% of A427 cells were infected when a multiplicity of infection equal to 10 was used for the Ad5-CMVhSSTr2 infection (data not shown). Assuming the 40% infection level is a maximum, and in vivo infection is only 10% as effective, then direct tumor injections of Ad5-CMVhSSTr2 (10^9 pfu) would infect an estimated 4×10^7 tumor cells ($0.4 \times 0.1 \times 10^9$). Assuming 1 P829 molecule binds per hSSTr2 receptor, then 10^{12} P829 molecules divided by 4×10^7 infected cells would equal 25,000 hSSTr2 receptors/cell. Further studies are necessary to determine the precise in vivo number of hSSTr2 receptors induced by Ad5-CMVhSSTr2. However, this work shows that in vivo imaging easily detected relatively limited hSSTr2-expressing cells in the A427 tumors.

Because mice were killed immediately after imaging, it was possible to compare imaging ROI analyses with the results of counting the tissues separately. There was excellent agreement between the 2 methods for uptake in the kidneys. However, when the tumor uptakes (%ID) as determined by imaging ROI analyses (Ad5-CMVhSSTr2-injected) were normalized to tumor weights, the calculated values (%ID/g) were higher than the results obtained when the tumors were removed and counted in a γ counter. Because the discrepancy was greatest for the smallest tumors, it is probably accounted for by leakage of the Ad5 vector outside of the tumor. The imaging would not distinguish between uptake in tumor and hSSTr2-positive cells immediately adjacent to the tumor—for example, the skin. However, skin was removed when the tumor was measured separately.

The retention of ^{99m}Tc-P829 and ^{188}Re-P829 in the Ad5-CMVhSSTr2-injected tumors was very similar. This similarity was also true for most other tissues, with the exception that ^{188}Re-P829 had slightly less binding in the liver and spleen. Overall, the highest uptake for both radiolabeled P829 peptides was in the kidney. Obviously, the high kidney clearance contributed to the low residual blood activity and therefore low background for imaging the hSSTr2-positive tumor cells. The high kidney uptake will not be a significant problem for most future human imaging applications because imaging modalities can distinguish this organ from other anatomic areas of interest. However, for therapy applications, the high kidney uptake will limit the maximum dose that can be administered. Also, lysine injections have been shown to lower the kidney uptake of other radiolabeled somatostatin analogs and antibodies (*32,33*).

Gene therapy vectors have been developed to encode 2 genes (*34,35*). Therefore, it is possible to construct a gene therapy vector that includes a gene to function only as a reporter for in vivo imaging, with simultaneous inclusion of a second therapy gene. We constructed this type of bicistronic adenoviral vector, combining the hSSTr2 gene with a second therapy gene encoding cytosine deaminase. Work is currently in progress to correlate ^{99m}Tc-P829 uptake with cytosine deaminase enzymatic activity. A second adenoviral vector encoding the hSSTr2 and HSTK genes has been produced. These vectors represent potential applications for the hSSTr2 gene as a reporter with the imaging capability provided by the ^{99m}Tc-P829 described in this article. An additional possibility is that the reporter gene may also function as a therapy gene. In this situation, ^{188}Re-P829 would offer the advantage of a strong β emission for therapy, while still allowing imaging with the 155-keV γ-ray emission.

Both ^{99m}Tc and ^{188}Re are produced from generator systems, which allow widespread distribution at relatively low cost. The particleless decay of ^{99m}Tc is an advantage for minimizing radiation dose, whereas the short half-life (6 h) would allow repeated evaluations. γ camera and SPECT imaging systems currently used in nuclear medicine are ideal for imaging both ^{99m}Tc and ^{188}Re. All of these advantages make this approach for imaging gene transfer particularly attractive. The system reported in this article is the first generation and, undoubtedly, future improvements will lead to increased sensitivity and accuracy.

CONCLUSION

The specific, localized expression of a reporter receptor in human tumor xenografts in mice after gene transfer with an adenoviral vector was detected by γ camera imaging and immunohistochemistry. Imaging the expression of the reporter hSSTr2 receptor with radiolabeled peptides has great potential for human applications, in particular for determining the targeting of gene therapy vectors.

ACKNOWLEDGMENTS

The authors greatly appreciate the encouragement from Dr. Larry Bush and Dr. Michael Azure and their generous supply of the P829 kits. The authors also thank Wu Qi, Zhu Min, Richard Kirkman, Sheila Bright, Christine Olsen, Debbie Della Manna, and Rob Stockard for excellent technical assistance. This research was supported in part by National Cancer Institute grant CA80104, National Institutes of Health grant CA73636, and Department of Energy grant DE-FG02–93ER61654.

REFERENCES

1. Wiebe LI, Morin KW, Knaus EE. Radiopharmaceuticals to monitor gene transfer. *Q J Nuc Med.* 1997;41:79–89.
2. Bogdanov A Jr, Weissleder R. The development of in vivo imaging systems to study gene expression. *Trends Biotechnol.* 1998;16:5–10.
3. Service RF. Molecular imaging: new probes open windows on gene expression, and more. *Science.* 1998;280:1010–1011.
4. Fehse B, Li Z, Schade UM, Uhde A, Zander AR. Impact of a new generation of gene transfer markers on gene therapy. *Gene Ther.* 1998;5:429–430.
5. Bennett J, Duan D, Engelhardt JF, Maguire AM. Real-time, noninvasive in vivo assessment of adeno-associated virus-mediated retinal transduction. *Invest Ophthalmol Vis Sci.* 1997;38:2857–2863.
6. Contag PR, Olomu IN, Stevenson DK, Contag CH. Bioluminescent indicators in living mammals. *Nat Med.* 1998;4:245–247.

7. Contag CH, Spilman SD, Contag PR, et al. Visualizing gene expression in living mammals using a bioluminescent reporter. *Photochem Photobiol.* 1997;66: 523–531.
8. Weissleder R, Tung CH, Mahmood U, Bogdanov A. In vivo imaging of tumors with protease-activated near-infrared fluorescent probes. *Nat Biotechnol.* 1999;17: 375–378.
9. Tjuvajev JG, Stockhammer G, Desai R, et al. Imaging the expression of transfected genes *in vivo*. *Cancer Res.* 1995;55:6126–6132.
10. Tjuvajev JG, Finn R, Watanabe K, et al. Noninvasive imaging of herpes virus thymidine kinase gene transfer and expression: a potential method for monitoring clinical gene therapy. *Cancer Res.* 1996;56:4087–4095.
11. Tjuvajev JG, Avril N, Oku T, et al. Imaging herpes virus thymidine kinase gene transfer and expression by positron emission tomography. *Cancer Res.* 1998;58: 4333–4341.
12. Alauddin MM, Conti PS, Mazza SM, Hamzeh FM, Lever JR. Synthesis of 9-[(3-[^{18}F]-fluoro-1-hydroxy-2-propoxy)methyl]guanine ([^{18}F]-FHPG): a potential imaging agent of viral infection and gene therapy using PET. *Nucl Med Biol.* 1996;23:787–792.
13. Alauddin MM, Conti PS. Synthesis and preliminary evaluation of 9-(4-[^{18}F]-fluoro-3-hydroxymethylbutyl)guanine ([^{18}F]FHBG): a new potential imaging agent for viral infection and gene therapy using PET. *Nucl Med Biol.* 1998;25:175–180.
14. Gambhir SS, Barrio JR, Wu L, et al. Imaging of adenoviral-directed herpes simplex virus type 1 thymidine kinase reporter gene expression in mice with radiolabeled ganciclovir. *J Nucl Med.* 1998;39:2003–2011.
15. Gambhir SS, Barrio JR, Phelps ME, et al. Imaging adenoviral-directed reporter gene expression in living animals with positron emission tomography. *Med Sci.* 1999;96:2333–2338.
16. Gambhir SS, Barrio JR, Hershman HR, Phelps ME. Assays for noninvasive imaging of reporter gene expression. *Nucl Med Biol.* 1999;26:481–490.
17. Shields AF, Grierson JR, Dohmen BM, et al. Imaging proliferation in vivo with [F-18]FLT and positron emission tomography. *Nat Med.* 1998;4:1334–1336.
18. Guenther I, Wyer L, Knust EJ, Finn RD, Koziorowski J, Weinreich R. Radiosynthesis and quality assurance of 5-[^{124}I]iodo-2′-deoxyuridine for functional PET imaging of cell proliferation. *Nucl Med Biol.* 1998;25:359–365.
19. Herschman HR, Sharfstein S, Gambhir SS, et al. In vivo imaging of gene expression associated with cell replication [abstract]. *J Nucl Med.* 1997;38:250P.
20. MacLaren DC, Gambhir SS, Satyamurthy N, et al. Repetitive, non-invasive imaging of the dopamine D_2 receptor as a reporter gene in living animals. *Gene Ther.* 1999;6:785–791.
21. Weissleder R, Simonova M, Bogdanova A, Bredow S, Enochs WS, Bogdanov A. MR imaging and scintigraphy of gene expression through melanin induction. *Radiology.* 1997;204:425–429.
22. Pearson D, Lister-James J, McBride W, et al. Somatostatin receptor-binding peptides labeled with technetium-99m: chemistry and initial biological studies. *J Med Chem.* 1996;39:1361–1371.
23. Vallabhajosula S, Moyer BR, Lister-James J, et al. Preclinical evaluation of technetium-99m-labeled somatostatin receptor-binding peptides. *J Nucl Med.* 1996;37:1016–1022.
24. Virgolini I, Leimer M, Handmaker H, et al. Somatostatin receptor subtype specificity and in vivo binding of a novel tumor tracer, ^{99m}Tc-P829. *Cancer Res.* 1998;58:1850–1859.
25. Blum JE, Handmaker H, Rinne NA. The utility of a somatostatin-type receptor binding peptide radiopharmaceutical (P829) in the evaluation of solitary pulmonary nodules. *Chest.* 1999;115:224–232.
26. Rogers BE, McLean SF, Kirkman RL, et al. In vivo localization of [^{111}In]-DTPA-D-Phe^1-octreotide to human ovarian tumor xenografts induced to express the somatostatin receptor subtype 2 using an adenoviral vector. *Clin Cancer Res.* 1999;5:383–393.
27. Falck-Pedersen E, Heinflink M, Alvira M, Nussenzveig DR, Gershengorn MC. Expression of thyrotropin-releasing hormone receptors by adenovirus-mediated gene transfer reveals that thyrotropin-releasing hormone desensitization is cell specific. *Mol Pharmacol.* 1999;45:684–689.
28. Knapp FF, Beets AL, Guhlke S, et al. Availability of rhenium-188 from the alumina-based tungsten-188/rhenium-188 generator for preparation of rhenium-188-labeled radiopharmaceuticals for cancer treatment. *Anticancer Res.* 1997;17: 1783–1796.
29. Knapp FF. Rhenium-188: a generator-derived radioisotope for cancer therapy. *Cancer Biother Radiopharm.* 1998;13:337–349.
30. Munson P, Rodbard D. Ligand: a versatile computerized approach for characterization of ligand binding systems. *Anal Biochem.* 1980;107:220–239.
31. Grizzle WE, Myers RB, Manne U, Stockard CR, Harkins LE, Srivastava S. Factors affecting immunohistochemical evaluation of biomarker expression in neoplasia. In: Hanausek M, Walaszek Z, eds. *John Walker's Methods in Molecular Medicine: Tumor Marker Protocols.* Totowa, NJ: Humana Press; 1998:161–179.
32. Bernard BF, Krenning EP, Breeman WA, et al. D-Lysine reduction of indium-111 octreotide and yttrium-90 octreotide renal uptake. *J Nucl Med.* 1997;38:1929–1933.
33. Behr TM, Sharkey RM, Sgouros G, et al. Overcoming the nephrotoxicity of radiometal-labeled immunoconjugates: improved cancer therapy administered to a nude mouse model in relation to the internal radiation dosimetry. *Cancer.* 1997;80:2591–2610.
34. Bramson J, Hitt M, Gallichan WS, Rosenthal KL, Gauldie J, Graham FL. Construction of a double recombinant adenoviral vector expressing a heterodimeric cytokine: in vitro and in vivo production of biologically active interleukin-12. *Hum Gene Ther.* 1996;7:333–342.
35. Emtage PC, Wan Y, Bramson JL, Graham FL, Gauldie J. A double recombinant adenovirus expressing the costimulatory molecule B7–1 (murine) and human IL-2 induces complete tumor regression in a murine breast adenocarcinoma model. *J Immunol.* 1998;160:2531–2538.